

Article

High-Rate Crystal/Polycrystal Dislocation Dynamics

Ronald W. Armstrong 

Department of Mechanical Engineering, University of Maryland, College Park, MD 20742, USA; rona@umd.edu

Abstract: The present report builds upon work recently published on crystal and polycrystal dislocation mechanics behaviors assessed, in part, in split-Hopkinson pressure bar (SHPB) and shock loading investigations. A connection between the flow stress dependencies on strain rate in the different tests had been established in the previous report, whereas additional results are assessed here for (1) relationship of the measurements to a nano-scale prismatic dislocation structure proposed to be generated at a propagating shock front and (2) further relationships between the modeled structure and corresponding thermal stress and strain rate sensitivity computations, including new evaluations of the engineering rate sensitivity parameter, $m = [\Delta \ln \sigma / \Delta \ln (d\epsilon / dt)]_T$. A comparison is made of m values approaching 1.0 for simulated dislocation mechanics results computed for tantalum crystals. Other (lower) m value comparisons involve recently determined higher shock stress measurements made on copper material at higher temperatures.

Keywords: split-Hopkinson pressure bar measurements; shock waves in plate impact and gas-gun impact measurements; shock-front dislocation model generations; dislocation mechanics parameters; constitutive equation predictions; strain rate sensitivity parameters

1. Introduction

The plastic flow strength levels, σ_ϵ , of single crystal and polycrystalline materials increase more strongly than would otherwise be expected in split-Hopkinson pressure bar (SHPB) tests performed at applied strain rates, $(d\epsilon/dt)$, of $\sim 10^4 \text{ s}^{-1}$ or higher. Initial σ_ϵ measurements had been reported for polycrystalline copper by Follansbee, Regazzoni and Kocks [1]. More recently, additional SHPB measurements were reported by Lea, Brown and Jardine [2] and compared with the work by Follansbee et al. Another favorable compilation of copper measurements was presented recently by Jia, Rusinek, Pesci et al. [3] as part of their study of the analogous high-strain-rate behavior exhibited in shear tests of 304 stainless steel material. The upturn in the strain-rate-dependent σ_ϵ was initially proposed to be due to the onset of a “phonon drag resistance” to the motion of individual dislocations. Such resistance was described theoretically to be paramount when the driving force for dislocation motion was higher than the thermal stress associated with dislocation blocking obstacles. For copper and related face-centered cubic (fcc) metals, the thermal obstacles at conventional strain rates are known to be dislocation intersections.

The determination of such strength properties at higher loading rates has practical and theoretical importance. For example, current energy-based, atomic fusion, research activities involve subjecting metals to their upper-limiting strength levels under extremely high-rate loading conditions. A current world-wide research activity is to obtain reliable constitutive equation predictions for metal performances under these conditions. Of particular interest is to quantitatively relate such material performances and the equations describing them to the atomic-scale dislocation mechanisms capable of providing a fundamental basis for understanding potentially applicable material strength properties and enhancing their utilization.

Armstrong, Arnold and Zerilli [4] first experimentally associated the strong upturn in σ_ϵ for the Follansbee et al. measurements with other substantially higher flow stress levels reported for shock wave impact experiments performed by Swegle and Grady [5].



Citation: Armstrong, R.W. High-Rate Crystal/Polycrystal Dislocation Dynamics. *Crystals* **2022**, *12*, 705. <https://doi.org/10.3390/cryst12050705>

Academic Editor: Xiaoxu Huang

Received: 14 March 2022

Accepted: 19 April 2022

Published: 16 May 2022

Publisher's Note: MDPI stays neutral with regard to jurisdictional claims in published maps and institutional affiliations.



Copyright: © 2022 by the author. Licensee MDPI, Basel, Switzerland. This article is an open access article distributed under the terms and conditions of the Creative Commons Attribution (CC BY) license (<https://creativecommons.org/licenses/by/4.0/>).

The different experiments were shown on a dislocation mechanics model basis also to be connected on a flow stress versus strain rate basis by means of a limiting condition being obtained in a thermal activation–strain rate analysis (TASRA) description. Very importantly, the value of the TASRA-determined thermal activation volume, v^* , that is to be described in detail in the present report was shown to be increasingly reduced for copper beginning at the upturn in the SHPB measurements and, to reach a limiting small value determined under shock loading, to be equal to the dislocation Burgers vector cubed, b^3 . The reduction in v^* was taken to be indicative of the flow stress upturn being caused by an enhanced rate of dislocation generation and consequent multiplication of dislocation intersections. The subject has been recently reviewed and updated [6]. Other connections were made with a number of parameters derived from simulated dislocation model descriptions of shock behavior. The present report extends the work to include a model description for shock-induced dislocation generation at the propagating shock front and to establish a relationship with the results obtained in other recently reported investigations. Additional parametric evaluations are assessed over a wider range in strain rates; in particular, computations are presented for the v^* -related engineering, strain rate sensitivity, parameter, $m = [\Delta \ln \sigma / \Delta \ln (d\varepsilon / dt)]_T$.

2. The Dislocation Mechanics of Rate-Dependent Deformation

Figure 1 provides a compilation of SHPB and shock measurements based on the recent work of Lea et al. [2] and including the previous Follansbee et al. and dislocation mechanics descriptions of high-rate deformations [6]. The open-diamond and filled-circle measurements from Lea et al. also include open-circle measurements made afterwards at the indicated strain rates to demonstrate that the strain hardening had been largely retained, as normally occurs for “shock hardening”. The approximately linear-fitted lower strain rate Lea et al. and Follansbee et al. measurements, in the latter case made at a compressive strain, $\varepsilon = 0.15$, are matched in the figure in each case with the face-centered cubic (fcc) form of the Z–A relationship for the flow stress, σ_ε , that is expressed as [7]

$$\sigma_\varepsilon = \sigma_{G\varepsilon} + B_0[\varepsilon_r(1 - \exp\{-\varepsilon/\varepsilon_r\})]^{1/2} \exp[-\alpha T] + k_\varepsilon \ell^{-1/2} \quad (1)$$

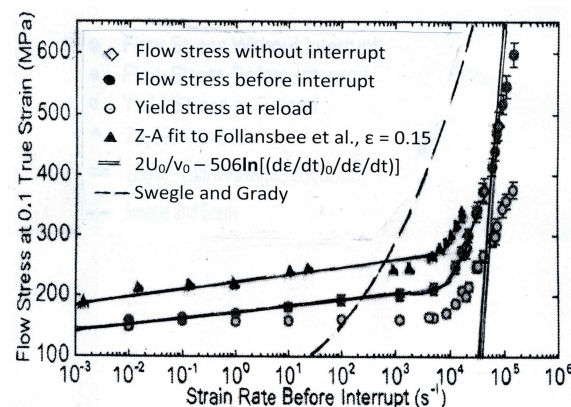


Figure 1. Comparison of Follansbee et al. [1], $\varepsilon = 0.15$, SHPB measurements fitted to a Z–A relationship [7] and follow-on $\varepsilon = 0.10$ measurements reported by Lea et al. [2], also shown in relation to extrapolation to the lower stress regime of experimental Swegle and Grady [5] and dislocation mechanics-based shock [4] descriptions.

In Equation (1), the σ_G term is attributed to athermal dislocation density and solute influences on the flow stress, B_0 is the thermal stress at absolute temperature $T = 0$, ε_r is a reference strain for dynamic recovery, $\alpha = \alpha_0 - \alpha_1 \ln(d\varepsilon / dt)$ for strain rate dependence, $(d\varepsilon / dt)$, and $k_\varepsilon \ell^{-1/2}$ is a Hall–Petch term for polycrystal grain size influence.

The strain rate enters into Equation (1) as $(d\varepsilon / dt)^{\alpha_1 T}$, for which $\alpha_1 = k_B / W_0$, k_B is Boltzmann’s constant, and $W_0 \approx 3.1 \times 10^{-20}$ J is a constant. On this basis, a dislocation

mechanics-based strain rate exponent, $m^* = k_B T / W_0$, is obtained in Equation (1) for the lower strain rate effect. As will be seen subsequently, it is important to distinguish between m^* for the specific thermal activation-based strain rate sensitivity and the determination of an m parameter for the total logarithmic dependence of stress on the logarithm of strain rate. Also in Figure 1, the dashed curve applies for the extension to lower stresses of the $\sigma_\epsilon = C(d\epsilon/dt)$ [1/4] relationship determined at higher shock pressures by Sweigle and Grady [5]. By comparison, the nearly vertical linear stress dependence applies for a dislocation mechanics prediction from the TASRA relation subject to assumption of a constant lower value of the activation volume parameter, $v^* = v_0$, being reached as expressed in the modified TASRA relationship [6]:

$$\sigma_\epsilon = (2U_0/v_0) - (2k_B T/v_0) \ln\{(d\epsilon/dt)_0/(d\epsilon/dt)\} \quad (2)$$

In Equation (2), U_0 is a reference Gibbs free energy at a highest strain rate, $(d\epsilon/dt)_0$, and k_B is Boltzmann's constant, 1.38×10^{-23} J. The limiting value of $v_0 \approx b^3$ determined from the dependence of σ_ϵ on $(d\epsilon/dt)$ had been determined for copper from the linear strain rate dependence shown in Figure 1. The reduced v^* value is attributed to a substantial increase in the dislocation density. Estimations of the $\{U_0, (d\epsilon/dt)_0\}$ parameters in Equation (2) are to be obtained in the present report.

2.1. The Thermal Activation Volume, $v^* = A^*b$

The TASRA-based thermal activation volume that corresponds to an activated slip area, A^* , multiplied by the dislocation Burgers vector is evaluated in experiments as

$$v^* = A^*b = k_B T [\Delta \ln(d\gamma/dt) / \Delta \tau_{Th}]_T \quad (3)$$

In Equation (3), $(d\gamma/dt)$ is the shear strain rate, equal to $m_T(d\epsilon/dt)$ through the Taylor orientation factor, m_T , and τ_{Th} is the thermal component of stress, equal to σ_{Th}/m_T , and is dependent on strain rate and temperature [8]. The dislocation model description of v^* is taken to be essentially dependent only on τ_{Th} . Figure 2 shows a recent (added-to) compilation of v^* versus τ_{Th} measurements including determinations for shock loading [6]. An inverse dependence of v^* on τ is indicated as

$$v^* = W_0 / \tau_{Th} \quad (4)$$

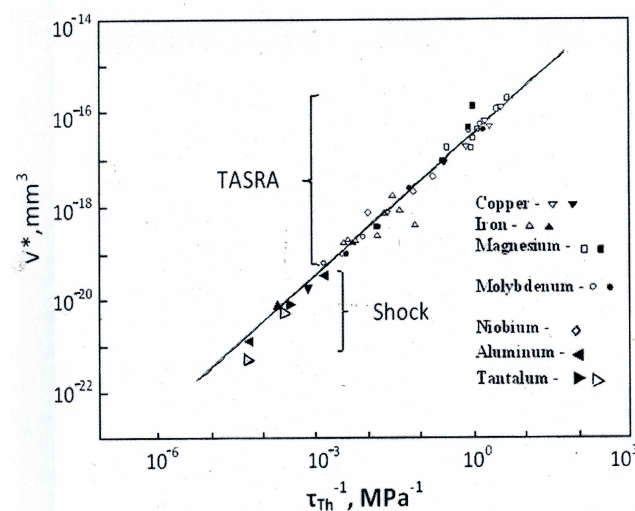


Figure 2. Thermal activation–strain rate analysis (TASRA) measurements of activation volume, $v^* = A^*b$, determinations for a variety of metals, as extended to include experimental shock test measurements [6] and incorporating (open-triangle) points for calculations based on simulated tantalum crystal shock results [9].

The constant $W_0 = 3.1 \times 10^{-20}$ J shown in Figure 2, as originally obtained from a plot of various conventional test measurements, is extended to include determinations for a number of shock measurements. The open-triangle points were determined from model dislocation simulations reported for shocked tantalum by Ravelo, Germann, Guerrero, An and Holian [9]. Very importantly, the parameter W_0 is seen also to be contained in the strain rate exponent factor described on a dislocation mechanics model basis in the text below Equation (1).

2.2. Higher Strain Rates—Smaller Shock-Induced Dislocation Loop Dimensions

Meyers, Jarmakani, Bringa and Remington [10] have described details of various dislocation structures associated with shock-induced deformations. In particular, a number of early models proposed for dislocation nucleations and their consequent arrangements were assessed. Meyers et al. pointed to experimental results obtained by Trueb [11] of a highest dislocation density of $\sim 10^{16} \text{ m}^{-2}$ being observed via transmission electron microscopy for a compressive stress of ~ 50 GPa applied to nickel material. Here, Figure 3a,b provide an additional model that was proposed to satisfy the ideal condition of one-dimensional strain being achieved at a propagating shock front [12,13]. The model was developed on the premise that a sufficiently high compressive strain imposed at all nano-dimensional points along the shock front could not be relaxed by the larger-scale micrometer displacement of a residual dislocation density [4,14]. Thus, the top-corner of Figure 3a provides a localized shear mechanism for the formation of a prismatic dislocation loop. Figure 3b shows a three-dimensional arrangement of such loops being intersected by an inclined slip plane. The shock hardening associated with “cutting through” such loops is suggested to relate to the post SHPB hardening depicted by Lea et al. [2] in Figure 1.

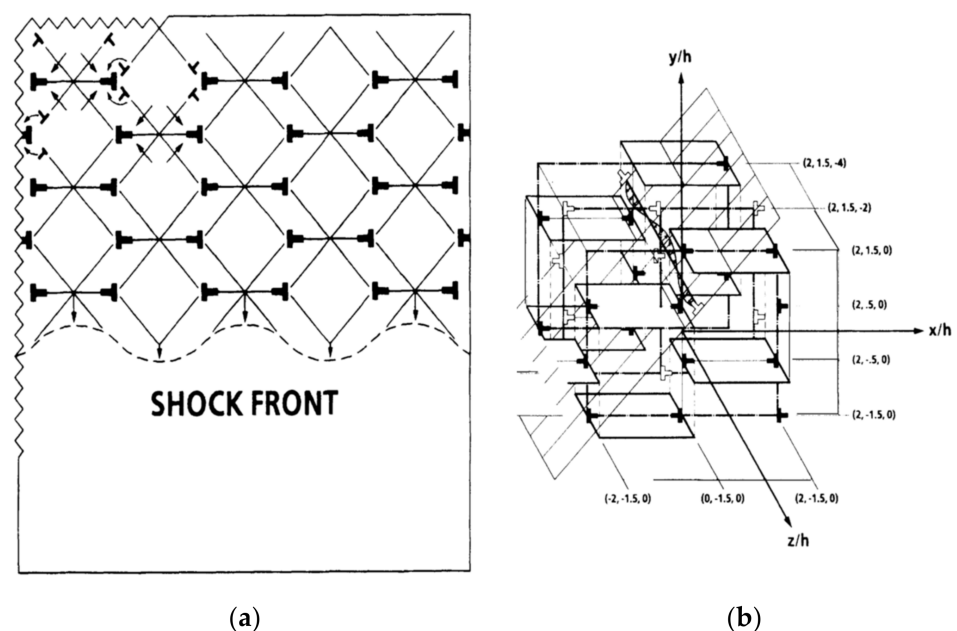


Figure 3. (a) Two-dimensional shock model for achievement of a one-dimensional state of compressive strain for a propagating shock wave [12]; (b) extension to a three-dimensional prismatic dislocation structure through which slip on an inclined plane would be restricted from cutting through the shocked nanostructure [13].

Germann, Tanguy, Holian, Lomdahl et al. have performed molecular dynamics (MD) calculations applied to the formation of periodic dislocation loop formations for $\langle 100 \rangle$ and $\langle 111 \rangle$ shock front propagations in a perfect copper crystal [15]. Zeretsky [16] has provided quantitative model calculations for an fcc crystal lattice of such a dislocation multiplication behind a shock front. Nano-scale partial dislocations separated in accordance with their

stacking fault energies were assessed for aluminum, nickel and copper crystals. A resultant dislocation structure not unlike that shown in Figure 3b was described. Most importantly, a characteristic time of 10^{-9} – 10^{-10} s was estimated for dislocation multiplication. The inverse time period provides an estimation of a highest strain rate, $(d\varepsilon/dt) = 10^{10} \text{ s}^{-1}$. Meyers et al. [10] have produced the same strain rate estimation. On this basis, Equation (2) for a limiting small value of v^* , as applied to Figure 2 and Equation (2), leads to a value of $U_0 = 5.4 \times 10^{-20}$ J. The calculated value of U_0 is not very different from the value of $W_0 = 3.1 \times 10^{-20}$ J, relating to Equation (4). Both values are taken to be representative of the Gibbs free energy for thermal activation at zero thermal stress.

3. Discussion

Agnihotri and Van der Giessen [17] have applied the method of discrete dislocation plasticity (DDP) to investigate the rate-dependent plasticity of copper leading from SHPB measurements to shock impacting. A comparison was made with the flow stress dependence on strain rate measured by Follansbee et al. [1]. The DDP simulation of the dislocation density produced at different applied strain rates in the range of 100 to $25,000 \text{ s}^{-1}$ was found to depend directly on the rate of dislocation generation. A generation rate, $(d\rho/dt) \approx 4.4 \times 10^{20} \text{ m}^{-2} \text{ s}^{-1}$, is computed at the highest strain rate to compare with a far higher rate of $(d\rho/dt) \approx 4 \times 10^{26} \text{ m}^{-2} \text{ s}^{-1}$ determined from the review by Meyers et al. [10] via multiscale dislocation dynamic plasticity (MDDP) simulations of shock propagation during tens of picoseconds in copper. Agnihotri and Van der Giessen also investigated the influences on rate sensitivity of thermal-type dislocation (blocking) obstacles, density of dislocation sources and grain size. A “dislocation drag” resistance for individual dislocation movement was included.

As mentioned earlier, such lattice phonon resistance, for example, becomes paramount when a dislocation is driven at a stress level above the barrier provided by TASRA-type obstacle resistance. Then, a direct proportionality of shear stress on strain rate obtains as demonstrated in the interpretation of gas-gun driven shock measurements made on copper [13,18]. Those measurements were obtained over a higher range in flow stresses between 8 and 20 GPa as compared to an upper stress level of ~ 3 GPa to be described in the present report and compared also to a much higher stress level of ~ 232 GPa for the high pressure solid state phase transformation of copper, not to downplay the importance of investigations of such higher stress-induced phase transformation studies. For copper, Luscher, Mayeur, Mourad, Hunter and Kenamond [19] have produced dislocation drag-based model calculations with higher phonon drag coefficients seemingly in agreement with the results presented in [13].

3.1. Extended Rate Dependence

Figure 4 shows an extended range of measurements and calculations based on evaluating the strain rate sensitivity dependence of plasticity in terms of the alternative engineering parameter, m , employed by Agnihotri and Van der Giessen [17] as

$$m = [\Delta \ln \sigma_\varepsilon / \Delta \ln (d\varepsilon/dt)]_T \quad (5)$$

In Equation (5), σ_ε is the total flow stress. It might be noted that the value of $m = m_T k_B T / v^* \sigma$, as related to Equation (3) and Figure 2, is a relatively complicated parameter.

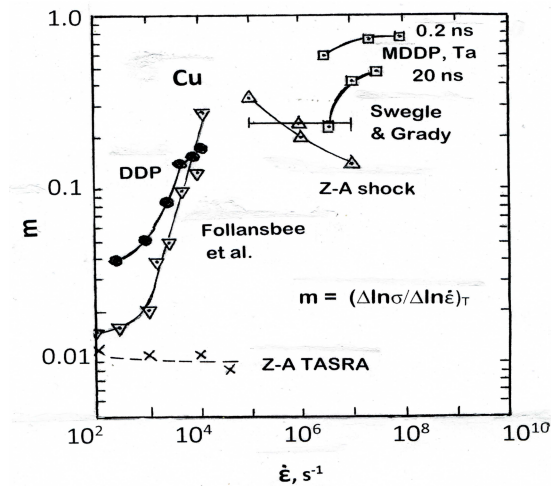


Figure 4. Computed strain rate sensitivity, $m = [\Delta \ln \sigma / \Delta \ln (d\epsilon/dt)]_T$, measurements and calculations for copper and tantalum materials covering a range of strain rates from SHPB to shock deformations [1,5,7,14,17,20].

In Figure 4, the open-triangle, Follansbee et al. [1], and filled circle, DDP, calculations of Agnihroti and Van der Giessen [17] are compared with crossed Z-A TASRA [7] and open-triangle, Z-A shock [13], as well as with Swegle and Grady [5] copper measurements and added open-square, MDDP calculations made for tantalum crystals [20]. The values of m were computed in accordance with the Equation (2) Z-A shock relationship as

$$m = [(U_0/k_B T) + (\ln\{[d\epsilon/dt]/[d\epsilon/dt]_0\})]^{-1} \quad (6)$$

Figure 4 shows, first, that a favorable comparison is obtained between the highest (calculated) DDP [17] and Follansbee et al. [1] SHPB results and the shock measurements [5,13]. The m values appear to be in agreement with strain-rate-dependent measurements reported for copper over a range in grain sizes by Mao, An, Liao and Wang [21]. Very interestingly, Mao et al. divide m into TASRA and viscous drag components on a constitutive equation basis. Of particular interest in Figure 4 are the MDDP calculations for tantalum crystals. The m values were computed directly from determination of the flow stress dependence on strain rate. Dislocation drag effects were included for the isentropic compression test simulations and for which the fastest rise time of 2×10^{-10} s compares favorably with the characteristic time period determined by Zaretsky [16] and by Meyers [10] for generation of a nano-scale dislocation structure. Armstrong et al. [13] had proposed a nano-scale twin structure to explain the value of v^* determined for shocked tantalum material.

3.2. Temperature Effect

Kanel, Savinykh, Garkushin and Razorenov [22] have reported flow stress measurements made on shock impact plate tests performed on annealed copper material at temperatures of 293, 983 and 1123 K. Figure 5 shows a comparison of the measurements with those previously described in the present report [1,5,13], compared also with Figure 1. An increase in the shock stress occurs for the higher temperature measurements. The results might be taken to show an effect of greater dislocation drag predicted at higher temperatures except for the very reasonable agreement shown with the pioneering measurements reported by Swegle and Grady [5] in which any drag consideration was excluded. A strain rate exponent, $m \approx 0.356$, < 1.0 for drag control, applies for the measurements. Additionally, the flow stresses are substantially lower than those interpreted as due to phonon drag in other gas-gun-induced shock measurements [13,18].

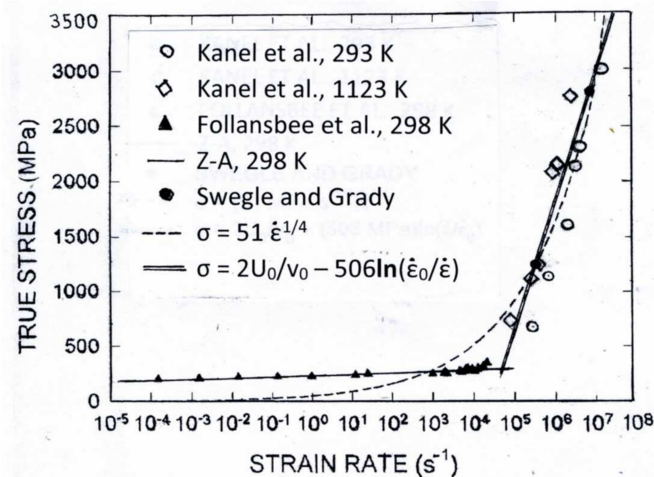


Figure 5. Temperature-dependent increase in shock-induced flow stresses obtained for annealed copper plate impact tests [20], as compared with Swegle and Grady plate impact measurements [5] and, at lower stresses, SHPB measurements of Follansbee et al. [1] fitted with a Z-A type fcc crystal constitutive relationship [6].

A possible influence on determination of the effective shock stress involving an increase in Poisson's ratio with increase in temperature has been suggested for the seemingly anomalous temperature effect. Measurements have been reported for Poisson's ratio increasing with an increase in pressure [23]. Kanel et al. [22] compared the temperature-dependent flow stress increase with the "normal" reverse temperature effect that was measured in their own SHPB tests. Very interestingly, they reported a reversal of the increased temperature effect in other measurements in which a small strain was initially present in the incident shock wave; so, the very interesting observation remains to be explained.

4. Summary

Split-Hopkinson pressure bar (SHPB) and shock impact measurements have been presented in relationship to other reported high-rate deformation test results and constitutive equation computations obtained on copper and tantalum materials. The total results are shown to compare reasonably quantitatively with a physical-based dislocation mechanics model description of dislocation generations at the shock front. On such a basis, a limiting form of the constitutive-equation-based thermal activation-strain rate analysis (TASRA) description is applied to shock behavioral predictions at an upper-limiting strain rate, $(d\varepsilon/dt) = 10^{10} \text{ s}^{-1}$. Additionally, a relationship is established with the engineering "log/log" strain rate sensitivity parameter, m , over a wide range in strain rates extending to the limiting value. The evaluation of constitutive equation parameters is related as well to simulated dislocation dynamics model descriptions for copper involving the method of discrete dislocation plasticity (DDP) and, for copper and tantalum, via the multiscale dislocation dynamic plasticity (MDDP) model.

Funding: This research received no external funding.

Institutional Review Board Statement: Not applicable.

Informed Consent Statement: Not relevant.

Data Availability Statement: Supporting data will be provided on request.

Conflicts of Interest: The author declares no conflict of interest.

References

1. Follansbee, P.S.; Regazzoni, G.; Kocks, U.F. The transition to drag-controlled deformation in copper at high-strain rates. In *Mechanical Properties of Materials at High Strain Rates*; Conference Series 70; Harding, J., Ed.; Institute of Physics: London, UK, 1984; pp. 71–80.
2. Lea, L.; Brown, L.M.; Jardine, A. Time limited self-organized criticality in the high rate deformation of face centered cubic metals. *Comm. Mater.* **2020**, *1*, 93–100. [[CrossRef](#)]
3. Jia, B.; Rusinek, A.; Pesci, R.; Bernier, R.; Bahi, S.; Bendarma, A.; Wood, P. Simple shear behavior and constitutive modeling of 304 stainless steel over a wide range of strain rates and temperatures. *Int. J. Impact Eng.* **2021**, *154*, 103896. [[CrossRef](#)]
4. Armstrong, R.W.; Arnold, W.; Zerilli, F.J. Dislocation mechanics of shock-induced plasticity. *Metall. Mater. Trans A* **2007**, *38*, 2605–2610. [[CrossRef](#)]
5. Swegle, J.W.; Grady, D.E. Shock viscosity and the prediction of shock wave rise times. *J. Appl. Phys.* **1985**, *58*, 692–701. [[CrossRef](#)]
6. Armstrong, R.W. Constitutive relations for slip and twinning in high rate deformations; A review and update. *J. Appl. Phys.* **2021**, *130*, 245103. [[CrossRef](#)]
7. Zerilli, F.J.; Armstrong, R.W. Dislocation mechanics based constitutive equation incorporating dynamic recovery and applied to thermomechanical shear instability. In *Shock Compression of Condensed Matter—1997*; Schmidt, S.C., Dandekar, D., Forbes, J.W., Eds.; American Institutes of Physics: New York, NY, USA, 1998; pp. 215–218.
8. Armstrong, R.W. Thermal activation strain rate analysis (TASRA) for polycrystalline metals. *J. Sci. Indust. Res.* **1973**, *32*, 591–598.
9. Ravelo, R.; Germann, T.C.; Guerrero, O.; An, Q.; Holian, B.L. Shock-induced plasticity in tantalum single crystals: Interatomic potentials and large-scale molecular-dynamics simulations. *Phys. Rev. B* **2013**, *88*, 134101. [[CrossRef](#)]
10. Meyers, M.A.; Jarmakani, H.; Bringa, E.M.; Remington, B.A. Dislocations in Shock Compression and Release. In *Dislocations in Solids*; Hirth, J.P., Kubin, L., Eds.; Elsevier B.V.: Amsterdam, The Netherlands, 2009; Volume 15, pp. 92–197.
11. Trueb, L.F. Electron-microscope study of thermal recovery processes in explosion-shocked nickel. *J. Appl. Phys.* **1969**, *40*, 2976–2987. [[CrossRef](#)]
12. Bandak, F.A.; Armstrong, R.W.; Douglas, A.S. Dislocation structure for one-dimensional strain in a shocked crystal. *Phys. Rev. B* **1992**, *46*, 3228–3235. [[CrossRef](#)] [[PubMed](#)]
13. Bandak, F.A.; Tsai, D.H.; Armstrong, R.W.; Douglas, A.S. Formation of nanodislocation dipoles in shock-compressed crystals. *Phys. Rev. B* **1993**, *47*, 11681–11687. [[CrossRef](#)] [[PubMed](#)]
14. Armstrong, R.W.; Arnold, W.; Zerilli, F.J. Dislocation mechanics of copper and iron in high rate deformation tests. *J. Appl. Phys.* **2009**, *105*, 023511. [[CrossRef](#)]
15. Germann, T.C.; Tanguy, D.; Holian, B.L.; Lomdahl, P.S.; Mareschal, M.; Ravelo, R. Dislocation structure behind a shock front in fcc perfect crystals: Atomistic simulation results. *Metall. Mater. Trans. A* **2004**, *35*, 2609–2615. [[CrossRef](#)]
16. Zaretsky, E. Dislocation multiplication behind the shock front. *J. Appl. Phys.* **1995**, *78*, 3740–3747. [[CrossRef](#)]
17. Agnihotri, P.K.; Van der Giessen, E. On the rate sensitivity in discrete dislocation plasticity. *Mech. Mater.* **2015**, *90*, 37–46. [[CrossRef](#)]
18. Jarmakani, H.; McNaney, J.M.; Kad, B.; Orlikowski, D.; Nguyen, J.H.; Meyers, M.A. Dynamic response of single crystalline copper subjected to quasi-isentropic, gas-gun driven loading. *Mater. Sci. Eng. A* **2007**, *463*, 249–262. [[CrossRef](#)]
19. Luscher, D.J.; Mayeur, J.R.; Mourad, H.M.; Hunter, A.; Kenamond, M.A. Coupling continuum dislocation transport with crystal plasticity for application to shock loading conditions. *Int. J. Plast.* **2016**, *76*, 111–129. [[CrossRef](#)]
20. Shehadeh, M.A.; El Ters, P.; Armstrong, R.W.; Arnold, W. Dislocation mechanics of extremely high rate deformations in iron and tantalum. *ASME J. Eng. Mater. Technol.* **2022**, *144*, 11015. [[CrossRef](#)]
21. Mao, Z.N.; An, X.H.; Liao, X.Z.; Wang, J.T. Opposite grain size dependence of strain rate sensitivity of copper at low vs. high strain rates. *Mater. Sci. Eng. A* **2018**, *738*, 430–438. [[CrossRef](#)]
22. Kanel, G.I.; Savinykh, A.S.; Garkushin, G.V.; Razorenov, S.V. Effects of temperature and strain on the resistance to high-rate deformation of copper in shock waves. *J. Appl. Phys.* **2020**, *128*, 115901. [[CrossRef](#)]
23. Hayes, D.; Hixson, R.S.; McQueen, R.G. High pressure elastic properties, solid-liquid phase boundary and liquid equation of state from release wave measurements in shock-loaded copper. In *Shock Compression of Condensed Matter—1999*; CP505; Furnish, M.D., Chhabildas, L.C., Hixson, R.S., Eds.; American Institutes of Physics: New York, NY, USA, 2000; pp. 483–488.